specimen current amplifier.

With further improvements in the design of the correction circuitry and in the setting-up procedure, it is believed that it will be possible to obtain adequate SACPs with $2\phi = 9°$ and from areas as small as 0.5 μm. For areas smaller than this, it will probably be necessary both to improve the final lens and also to use a brighter electron source, compared with the standard tungsten hair-pin filament used here, in order to obtain sufficient probe current to observe the channelling contrast.

Acknowledgements

The authors are indebted to Dr G. R. Booker for suggestions and discussions, and to Dr C. G. van Essen for discussions and technical advice.

References

1. C. G. VAN ESSEN, E. M. SCHULSON, and R. H. DONAGHAY, *Nature*, **225** (1970) 847, and *J. Mater. Sci.* **6** (1971) 213.
2. C. G. VAN ESSEN and E. M. SCHULSON (to be published).
3. G. R. BOOKER and R. STICKLER, *J. Mater. Sci.* **7** (1972) 712.
4. C. G. VAN ESSEN, Proc. 25th Anniversary Meeting EMAG (Institute of Physics) Cambridge (1971) p. 314

Received 20 December 1971
and accepted 24 February 1972

D. C. JOY
D. E. NEWBURY
Department of Metallurgy
University of Oxford
England

An aluminium—α-alumina composite

The recent availability of single-crystal α-alumina in filamentary form [1] has resulted in marked interest in the use of this materal as a reinforcing agent in metal-matrix composites [2-3]. Apart from having excellent mechanical properties (tensile strength ~ 2000 MN/m^2 and modulus of ~ 4.65×10^5 MN/m^2), these filaments have been shown to exhibit good stability in metal matrices up to temperatures of ~ 1373 K [2].

The present programme was aimed at studying some of the mechanical characteristics of alumina filaments embedded in an aluminium matrix. For effective reinforcement, the length of fibre embedded in matrix material must exceed a critical value (l_c), given by the equation [4]:

$$\frac{l_c}{d} = \frac{\sigma_f}{2\tau_y} \tag{1}$$

where d is the fibre diameter, σ_f the fracture stress of the fibre, and τ_y the shear stress of the fibre/matrix interface. Values of the critical aspect ratio (l_c/d) have been determined by casting aluminium around single filaments and performing draw-out tests similar to those described by Kelly and Tyson for metal wires embedded in various metal matrices [5-6].

Materials used in the present study were 0.51 mm diameter filaments of single crystal α-alumina, and high purity (99.999%) aluminium. The technique used to produce the composite specimens involved casting the aluminium at a temperature of 1073 K into a graphite mould containing the alumina filament. This technique, which is described in detail elsewhere [7], resulted in good filament alignment and interfacial bonding.

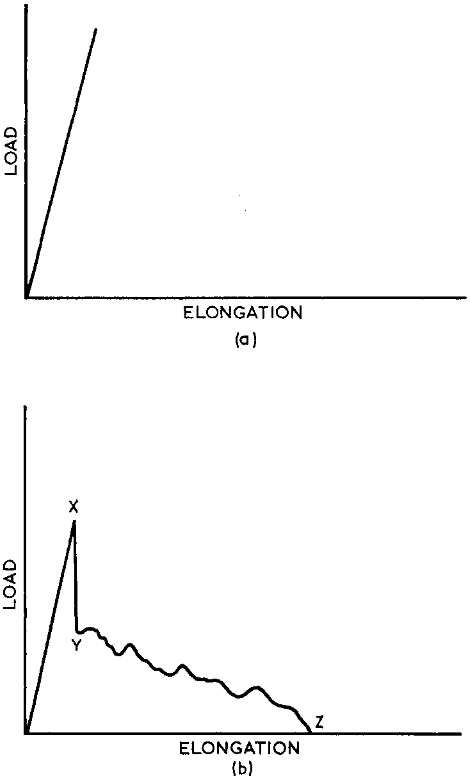

Figure 1 Typical load-extension plots for specimens exhibiting (a) fibre fracture, and (b) fibre pull-out.

Tensile testing of composite specimens at 293 K resulted in either filament fracture ($l > l_c$) or filament pull-out ($l < l_c$). A typical load-extension curve for specimens exhibiting the former is shown in Fig. 1a. The mean filament fracture stress of 2045 MN/m^2 was in good agreement with previously quoted values for this material [1]. Fracture-surface appearances were typical of those associated with high-strength ceramic fibres [8], and consisted of a fracture-initiation zone adjacent to the edge of the filament and radial cleavage facets.

The 0.2% proof stress and UTS values obtained at 293 K from tensile tests on specimens machined from the as-cast matrix material were 36.29 MN/m^2 and 47.39 MN/m^2 respectively.

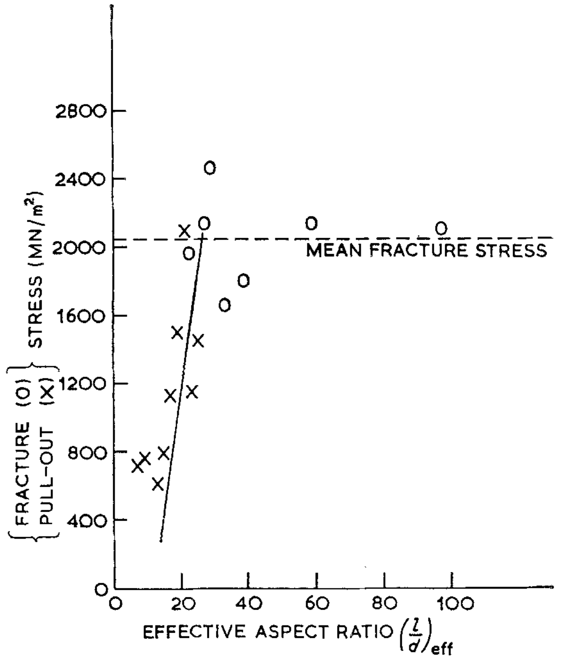

Figure 2 Effect of aspect ratio on filament pull-out or fracture stress.

The general form of the load-elongation curve for specimens which exhibited filament pull-out is shown in Fig. 1b. The stress at which pull-out was first detected (X) increased with the length of filament embedded until the critical length was reached. The results of these tests are presented in Fig. 2, where the pull-out or fracture stress is plotted against the effective aspect ratio. (The parameter $(l/d)_{\text{eff}}$ applies to the case of a fully embedded filament, i.e. for a simple pull-out test, $l = 0.5\, l_{\text{effective}}$.) It will be seen from Fig. 2 that the alumina filaments exhibit a critical aspect ratio of $\sim$ 26.

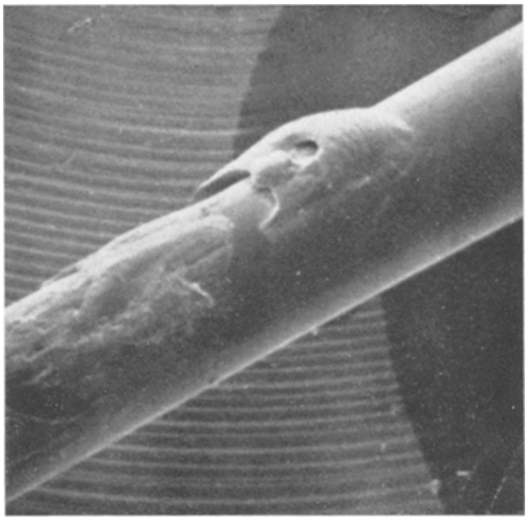

Figure 3 Layer of matrix aluminium on filament surface after pull-out. Magnification: × 50.

Filaments which were pulled out from the matrix material retained some aluminium on the filament surface, an effect illustrated in Fig. 3. Examination of these filaments at high magnification indicated that the aluminium layer often exhibited markings parallel to the pull-out direction (Fig. 4). It would appear from these observations that the mechanism of filament pull-out involved not only filament/matrix decohesion, but also shear failure of the surrounding matrix material. This mixed mode of filament pull-out was reflected in the load-elongation curves (Fig. 1b) and it is suggested that the initial load drops (XY) were a consequence of matrix/filament decohesion and that this was followed by shear failure in the aluminium matrix to produce complete pull-out (YZ). The average thickness of the aluminium layer on the alumina filaments (Fig. 3) was $\sim$ 4μm. This was determined by weighing the filaments before and after dissolving the aluminium from the filament. Mass spectrographic analyses of alumina filaments, the aluminium-matrix material, and a pulled-out filament are presented in Table I.

From the results of Fig. 2, a value of 34 MN/m^2 for the shear strength of the fibre-matrix interface was obtained. This result is in general agreement with those previously reported from shear tests on sessile drop-type specimens [9]. It

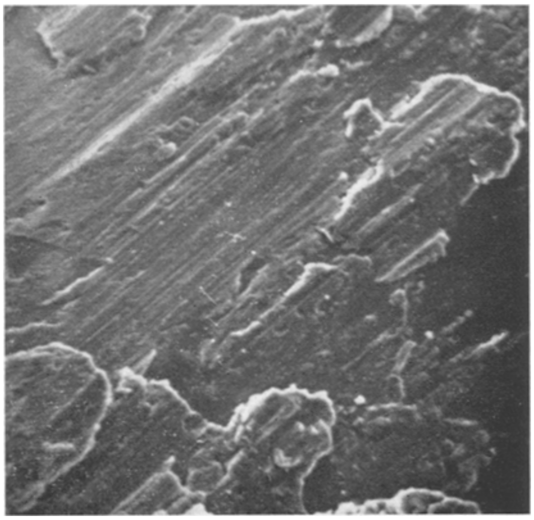

Figure 4 Shear markings on layer of matrix material after pull-out. Magnification: × 333.

is interesting to note that in previously reported work on the fracture of aluminium-alumina composites, there is evidence of considerable shear in the aluminium away from the metal ceramic interface [9].

The results of Champion *et al* [10-11] indicated that the contact angle between alumina and aluminium decreased with increasing temperature and that the condition for wetting was reached at ~ 1323 K. In the present experiments the aluminium at a temperature of 1073 K was cast around the filaments. Clearly, an interface shear strength of 34 MN/m^2 indicates good bonding of the composite although the casting temperature was nominally too low to result in wetting between the two components. An indication of the nature of the bond may be found in the results in Table I. Compared with columns A and B the general impurity level in column C was much higher. This may have occurred due to the segregation of impurities to the alumina/metal interface during solidification of the aluminium matrix. It may also be partly due to variations in absolute levels of impurity content as a consequence of the small samples analyzed by this technique. Accepting this limitation, the results do indicate an increase in the concentration of elements such as Na, K and Si in the region of the filament-matrix interface. The oxides of these elements could be expected to react readily with alumina and form the basis of a chemical bond. The casting procedure was carried out in laboratory air and the availability of excess oxygen may have contributed to the ease with which a chemical bond was obtained.

TABLE I Mass spectrographic analysis of alumina filaments and matrix aluminium (ppm by wt).

Element	A	B	C
Ag	1.6	—	6.0
Cu	1.2	0.4	4.5
Zn	0.8	2.0	4.0
Ni	1.8	—	3.0
Fe	8.8	2.2	33.0
Cr	1.0	0.2	3.6
Ti	25.0	0.3	36.0
Ca	12.0	0.2	60.0
K	20.0	0.3	45.0
Cl	26.0	6.5	80.0
S	6.0	1.0	210.0
P	1.2	1.0	10.0
Si	18.0	15.0	96.0
Na	20.0	1.0	200.0
F	2.0	2.0	100.0
Sn	—	6.0	0.4
Mg	—	40.0	90.0

A Alumina filament.
B Aluminium-matrix material.
C Filament with aluminium layer from pull-out test.

Acknowledgments

This work was carried out in the Department of Physical Metallurgy and Science of Materials, University of Birmingham, whilst one of the authors, (D.I.G.) held the Chubb Fellowship. The authors wish to thank Messrs Chubb Ltd. for their interest in the programme and Professor R. E. Smallman for the provision of laboratory facilities.

References

1. Tyco Laboratories Inc., Waltham, Massachusetts 02154, Bulletin No. 103.
2. J. E. RESTALL, A. BURWOOD-SMITH, and K. F. A. WALLES, *Metals and Materials*, **4** (1970) 467.
3. R. E. TRESSLER and T. L. MOORE, *Metals Eng. Quart.* (1971) 16.
4. A. KELLY and G. J. DAVIES, *Met. Rev.* **10** (1965) No. 37.
5. A. KELLY and W. R. TYSON, in "High Strength Materials" (ed. V. F. Zackay) (John Wiley and Son, Interscience, New York, 1965) p. 578.
6. *Idem, J. Mech. & Phys. Sol.* **13** (1965) 329.
7. D. I. GOLLAND and C. J. BEEVERS, Chubb Research Report, Dept. of Physical Metallurgy, University of Birmingham (1970)—copies available on request.
8. W. D. KINGERY, "Introduction to Ceramics" (J. Wiley, New York, 1970) p. 606.

9. M. NICHOLAS, *J. Mater. Sci.* **3** (1968) 571.
10. J. A. CHAMPION, B. J. KEENE, and J. M. SILLWOOD, *ibid*, **4** (1969) 39.
11. *Idem*, *ibid*, **4** (1969) 1111.

Received 26 January
and accepted 22 February 1972

D. I. GOLLAND*
C. J. BEEVERS
Department of Physical Metallurgy
and Science of Materials
University of Birmingham
Birmingham, England

---

*Now at: Department of Materials Engineering, North Carolioa State University, Raleigh, North Carolina 27607, USA.

Induced growth anisotropy in TGS crystals

Crystals of ferroelectric triglycine sulphate (TGS) are currently of interest for use in infrared imaging and detection devices, and the controlled growth of large crystals has received considerable attention.

The pure material usually grows with antiparallel arrays of ferroelectric domains which can be displayed by various techniques, including decoration by vacuum evaporation of tellurium on to freshly cleaved surfaces [1]. Single domain specimens can readily be formed by polarizing fabricated crystal specimens by the application of relatively low fields, of the order of 200 V cm^{-1} The material is, however, subject to depolarization by thermal, mechanical or electrical means and great interest has resulted from the discovery that crystals doped with small concentrations ($\sim 1\%$) of L-alanine result in a built-in bias which can only be reversed by application of a large field.

In the controlled programmed growth of the doped (LATGS) crystals from aqueous solution, a curious phenomenon was noted. The growth technique used involves placing seed crystals, prepared from cleaved slices, on a perspex shelf in such a manner that only one "half" of a crystal develops. Starting with undoped TGS seeds in L-analine doped solution, it was noted that all crystals grew in an elongated manner along the *c*-axis, as reported by Lock [2], but some were also elongated along the *b*-axis, while others grew in a truncated form. Subsequent experiments with doped seeds confirmed that the difference in form was related to the orientation of the seed and depended on whether the 010 or $0\bar{1}0$ plane was exposed to the solution. Crystals grown along the two directions are shown in fig. 1, the lower crystal (inverted for the photograph) corresponding to growth on the $0\bar{1}0$ plane. This confirms that the alanine molecules are stereo-specifically adsorbed on to the crystal surface and are incorporated into the crystal in a precise orientation and indicates that the built-in bias occurs without the necessity of using single-domain seed crystals.

One other difference noted between the two forms of crystal was that truncated crystals were badly strained and tended to shatter either during growth or on cooling to room temperature at the termination of the run. This occurred when both forms of crystal were grown in the same tank under identical conditions of supersaturation. The tall-form crystals were unstrained and showed no unusual defects even though the linear growth rate was approximatly 1.5 × that

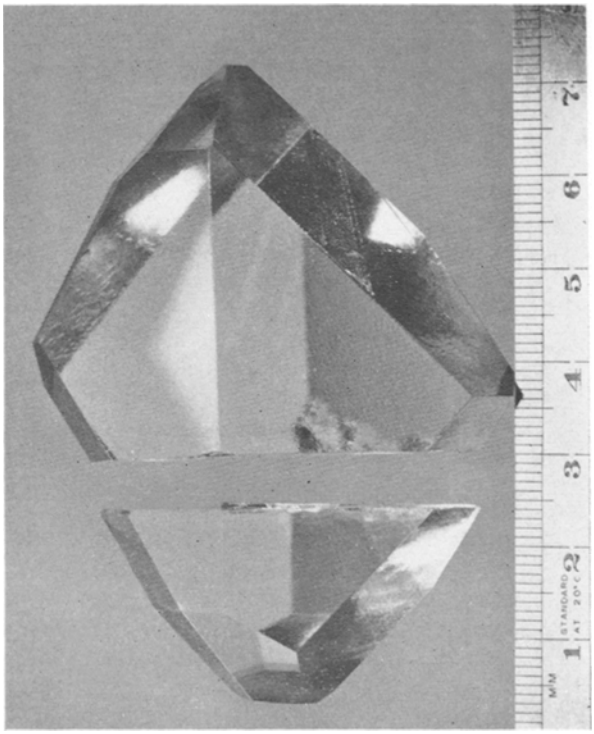

Figure 1 Tall and short habit crystals of LATGS.